Development of metal hydride surface structures for high power NiMH batteries
Also extended cycle-life and lead to more effective recycling methods

Yang Shen

Abstract
By combining alkaline etching of hydrogen storage alloys or their hydrides with a controlled oxidation, it was possible to improve reaction kinetics and accelerate activation of MH-electrodes. Both AB_5 and AB_2 alloys were studied where A is mixtures of rare earth elements for AB_5 alloys and titanium and/or vanadium, zirconium for AB_2 alloys; nickel contributes the major part of B. With SEM and TEM studies the surface could be described as consisting of several phases where an interphase with active Ni-containing cluster protected the inner metallic hydrogen storage part of the powder particles. These catalytic Ni-clusters presumably lead to the fast activation and high discharge capacity of alloy.

This interphase was observed to be stable enough to allow us to develop a method, where we could add pure oxygen to a NiMH battery pack in order to regenerate the amount of electrolyte that was lost during long time cycling of the battery. Meanwhile, the method will rebalance the electrodes mitigating excessive pressures during over charge. Therefore, the internal resistance of cells can be reduced and cycle life will increase.

It was also shown that the stable interphase could survive a mild ball milling or sonication which enabled us to upcycle material from spent NiMH batteries into a better working MH-electrodes with improved kinetics and activation properties. Reuse of ball-milled or sonicated material could serve as a simple recycling alternative to energy-demanding metallurgical smelting methods and chemical consuming hydrometallurgical recycling processes, where the possibilities of up-scaling further favour the less complex mechanical treatments. The stable but catalytic interphase protecting the inner particles indicates that the MH-electrode material may perform better in its second life in a new NiMH battery.

Keywords: *Metal hydrides, NiMH batteries, Surface treatment, Ni clusters, Rare earths hydroxides, Oxygen, Hydrogen.*

Department of Materials and Environmental Chemistry (MMK)

Stockholm University, 106 91 Stockholm

DEVELOPMENT OF METAL HYDRIDE SURFACE STRUCTURES
FOR HIGH POWER NIMH BATTERIES

Yang Shen

Development of metal hydride surface structures for high power NiMH batteries

Also extended cycle-life and lead to more effective recycling methods

Yang Shen

Development of metal hydride surface structures for high power NiMH batteries also extended cycle-life and lead to more effective recycling methods.

Abstract

By combining alkaline etching of hydrogen storage alloys or their hydrides with a controlled oxidation, it was possible to improve reaction kinetics and accelerate activation of MH-electrodes. Both AB_5 and AB_2 alloys were studied where A is mixtures of rare earth elements for AB_5 alloys and titanium and/or vanadium, zirconium for AB_2 alloys; nickel contributes the major part of B. With SEM and TEM studies the surface could be described as consisting of several phases where an interphase with active Ni-containing cluster protected the inner metallic hydrogen storage part of the powder particles. These catalytic Ni-clusters presumably lead to the fast activation and high discharge capacity of alloy.

This interphase was observed to be stable enough to allow us to develop a method, where we could add pure oxygen to a NiMH battery pack in order to regenerate the amount of electrolyte that was lost during long time cycling of the battery. Meanwhile, the method will rebalance the electrodes mitigating excessive pressures during over charge. Therefore, the internal resistance of cells can be reduced and cycle life will increase.

It was also shown that the stable interphase could survive a mild ball milling or sonication which enabled us to upcycle material from spent NiMH batteries into a better working MH-electrodes with improved kinetics and activation properties. Reuse of ball-milled or sonicated material could serve as a simple recycling alternative to energy-demanding metallurgical smelting methods and chemical consuming hydrometallurgical recycling processes, where the possibilities of up-scaling further favour the less complex mechanical treatments. The stable but catalytic interphase protecting the inner particles indicates that the MH-electrode material may perform better in its second life in a new NiMH battery.

Keywords: *Metal hydrides, NiMH batteries, Surface treatment, Ni clusters, Rare earths hydroxides, Oxygen, Hydrogen.*

List of Papers

This thesis is based on the following papers, which are referred to the roman numbers.

Paper I: Shen Y, Peng F, Kontos S, Noréus D. Improved NiMH performance by a surface treatment that creates magnetic Ni-clusters. International Journal of Hydrogen Energy 2016;41: 9933-9938.

My contribution: I planned and executed all experimental work. I wrote the manuscript. I did most characterizations expect the TEM part was performed by the second author and the magnetization part was done by the third author.

Paper II: Tan S, Shen Y, Şahin, EO, Noréus D, Öztürk T. Activation behavior of an AB_2 type metal hydride alloy for NiMH batteries. International Journal of Hydrogen Energy 2016;41: 9948–9953.

My contribution: I planned the work with first author and did the KOH treatment part. I was involved in the writing and discussions about the manuscript.

Paper III: Shen Y, Noréus D, Starborg S. Increasing NiMH battery cycle life with oxygen. International Journal of Hydrogen Energy 2018;43: 18626-18631.

My contribution: I planned and executed all experimental work. I did all characterizations. I wrote most of the manuscript.

Paper IV: Shen Y, Grape E, Noréus D, Widenkvist E, Starborg S. Upcycling of spent NiMH battery material - Reconditioned battery alloys show faster activation and reaction kinetics than pristine alloys as well as longer cycle life due to lower corrosion rates. In Manuscript.

My contribution: I planned and executed the experimental work together with the second author. I wrote the manuscript.

Contents

1. Introduction

Nickel–metal hydride battery (NiMH) is a rechargeable type battery related to nickel–cadmium (NiCd) battery. Both NiMH and NiCd use the $Ni(OH)_2/NiOOH$ redox couple as counter electrode. But instead of Cd the NiMH battery uses hydrogen absorbed in a metal hydride. The volumetric hydrogen storage capacity in a metal hydride is almost twice as of that of the liquid hydrogen. NiMH batteries can double the capacities of NiCd for the equivalent size, and its volumetric energy density is comparable to some lithium-ion chemistries. Recycling efficiency is better than lithium-ion batteries. It is one of the most environmentally friendly rechargeable batteries. NiMH was commercialized at the end of 1980s and are widely used in hybrid electric vehicles and consumer electronics.[1-4] The automotive industry use of batteries will increase significantly with the introduction of various hybrid solutions for the power trains (Micro- and mild- and full hybrids). In these applications the NiMH battery chemistry is well suited. AB_2 AB_5 and A_2B_7-type hydrogen storage alloys are used as materials for the negative metal hydride electrode in NiMH. Most common are AB_5-type alloys, where A is mixtures of rare earth elements, B is mainly nickel. In AB_2-type alloy, A is titanium and/or vanadium, zirconium, with nickel as the major part of B. Generally, AB_2-type alloys have higher discharge capacity than AB_5-type, however, the reaction response of AB_2-type alloy is slow and they are more easily corroded and passivated. Newly developed La-Mg-Ni-based A_2B_7-type hydrogen storage alloys have high discharge capacity and good activation performance properties. One important advantage is that A_2B_7 alloys can be made without cobalt which has become expensive as it is a fairly rare metal used in Li batteries. The development of alternative materials with high total discharge capacity, good high-rate kinetics and long cycle stability is necessary to improve the performance of NiMH. The electropositivity of the A-elements makes them easy to be corroded in the alkaline electrolyte used in NiMH batteries. To inhibit corrosion it is important to form a thin protective layer on the alloy particles. This usually forms during the initial formation of the NiMH batteries, during which the alloy particle cracks up into smaller particles and fresh surface is exposed to the electrolyte. A small fraction of the electropositive metals in the surface is corroded liberating nickel that forms small clusters.[5-8] These clusters are presumed to be responsible for improving the reactions that transfer hydrogen in and out of the alloy particles.[5] They also show a complicated magnetic behaviour combining para-, ferro- and superparamagnetism.

Höganäs AB and Stockholm University have developed an alkaline surface treatment method that improves the reaction kinetics and corrosion stability of conventional NiMH battery AB_5-alloys.[9] A basic understanding of the phenomenon is, however, lacking. With this PhD project, we want to increase this understanding, which will form the basis for an extension of the method to include other more available metals, which can be used in batteries. The PhD project is done together with Höganäs AB, for the development of new materials; Nilar AB in Gävle, where the batteries are manufactured and Scania in Södertälje, where the batteries are tested. So the project is planned in close collaboration with industrial partners including the characterization of metal hydrides in an electrochemical environment.

This thesis is focusing on metal hydride electrodes. By following the development of the magnetization and correlate it to the polarization of the electrodes, we can obtain clues about the reaction paths at the surface. In this work, a surface treatment was used to improve kinetics at surface of metal hydrides. The treatment comprises three steps: decrepitating the alloy by cycling it using hydrogen gas; oxidizing the obtained hydride alloy powder and boiling the oxidized powder in an aqueous potassium hydroxide solution. Composition and surface morphology of the alloy after surface

treatment were studied by EDS, SEM, XPS, BET and TEM. Electrochemical characterization was investigated in half-cell test. For Magnetic properties of different samples were also measured. The electrochemical performance correlated to magnetic clusters in metal hydride surfaces after surface treatment is discussed. The goal of this work is to increase the understanding of the surface treatment, which will form the basis for an extension of the method to include other more available metals, which can be used in batteries. [paper I II]

Although NiMH batteries have long cycle life, the corrosion of the metal hydride from some negatively interacting processes reduces the amount of metal hydride capacity. More severely it consumes water in the electrolyte resulting in increased internal resistance, which is the main cause for cell failure. The corrosion, further, evolves hydrogen, causing an unbalance between the anode and the cathode, leading to the internal pressure increase at the end of charging, which accelerates the drying out of electrolyte if they vent through the safety valve. Both oxygen and hydrogen are added to a NiMH battery to compensate for the loss to hydroxide ions OH- formed in the corrosion process. A proper optimization of the gas additions combined with a cell design including an excess amount of MH-alloy to compensate for the corrosion can substantially increase the cycle life of NiMH batteries. [paper III]

Recycling of batteries in order to avoid pollution, reduce material cost and increase utilization is highly demanded. Mechanical as well as chemical treatments have been tested to recover hydrogen storage alloys from spent NiMH batteries. The treatments aimed to partially remove the outer corroded surface of the alloy particles while keeping its catalytic properties. In this study, we disassembled discharged bipolar NiMH battery modules produced by Nilar AB in Sweden after the modules have been used for long time testing and collected the spent MH-electrodes. The mechanical treatment were sonification and ball milling combined with a simple washing of the resulting mixture. The chemical treatments were acid- and alkaline washings. [paper IV]

1.1 Metal Hydride

Metals can be bonded to hydrogen to form new compounds i.e. metal hydrides. They are formed based on ionic, metallic or covalent bonds. Here I focus on metallic metal hydrides for NiMH batteries application. These intermetallic compounds can be broadly classified into six categories based on A-B component systems as: AB, AB_2, A_2B, A_2B_7, AB_3 and AB_5, where A are electropositive metals usually containing rare earth elements, Ti etc. Non or weakly hydride-forming metals as Ni, Fe etc. constitutes the major part of B which can be alloyed with Al, Co, Mg and Mn to achieve the targeted performance.[10,11] Table 1.1 shows examples of different types of alloys.

Table 1.1 Examples of intermetallic hydrides.

Composition	Compounds
AB	TiNi, TiFe, ZrNi
AB_2	$ZrMn_2, ZrV_2$, $TiMn_2$
A_2B	Mg_2Ni, Mg_2Co
AB_3	$NdCo_3$, $GdFe_3$
AB_5	$LaNi_5$, $CeNi_5$
A_2B_7	Pr_2Ni_7, Ce_2Co_7

The hydrogen volumetric capacity for metal hydride is normally high, in some cases twice that of liquid hydrogen, but the gravimetric capacity is low (< 4 wt. % hydrogen). The hydrogen absorption and desorption reaction for metal hydride can be written as:

$$2M\,(s) + xH_2\,(g) \rightleftharpoons 2MH_x\,(s) + Q \tag{1.1}$$

Here M is an intermetallic compound, MH_x is the corresponding hydride and x the ratio of hydrogen to metal and Q is the heat of reaction. When the metal hydride forms by absorbing hydrogen, heat is released, Q. The reverse process is an endothermic reaction requires a supply of the same amount of heat. [12]

1.2 Phase equilibria in the metal–hydrogen systems

Equilibrium of the hydrogen absorption and desorption reaction (1.1) can be characterised by PCT-diagram (Figure 1.1) which refers to an interrelation between hydrogen at a pressure (P), concentration of hydrogen in the solid phase (C) and temperature (T). In Figure 1.1, the x- and y-axes represent the concentration of hydrogen in the solid phase and hydrogen pressure, respectively. The metal hydride alloy absorbs hydrogen, in a 3-step process, hydrogen dissociates on the metal surface, H atoms diffuse into the bulk and start to form a solid solution region. This starts with an α-phase. In a metal host lattice, H atom is normally located inside a tetrahedron formed by four metal atoms or an octahedron surrounded by six metal atoms. In general, this will lead to an expansion of unit cell volume of about 2 to 3Å^3 per hydrogen atom. As hydrogen concentration increases, the hydride phase β grows. The α→β phase transition, exhibits an equilibrium plateau α+β region. The plateau width is often considered as the reversible hydrogen capacity of a material. After complete conversion from α-phase to β-phase, further absorption of hydrogen can be accompanied only by a significant increase of pressure. Multiple equilibrium plateaus can be observed if more hydride phases occur. The logarithm of the plateau pressure P can be plotted vs 1/T as a straight line according to the van't Hoff equation (1.2):

$$\ln P = -\frac{\Delta H}{RT} + \frac{\Delta S}{R} \tag{1.2}$$

Where R is gas constant, T is temperature, ΔH and ΔS are the enthalpy and entropy of hydride formation respectively. The enthalpy and entropy specify the working temperatures and the respective plateau pressures of the hydrides, which is an important measure of the stability of the hydrogen storage.
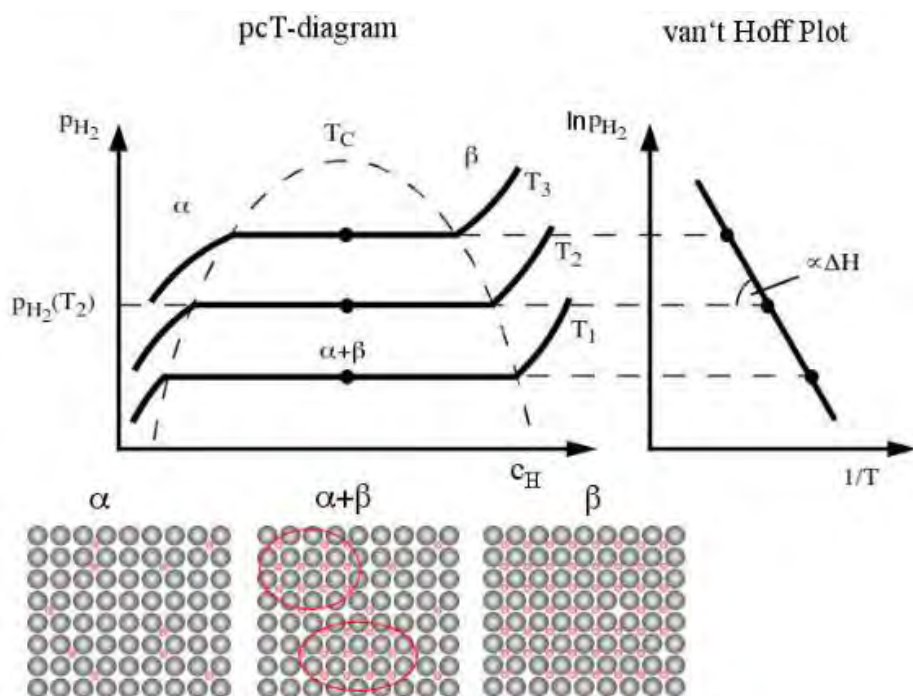
Figure 1.1 Schematic PCT-diagram and van't Hoff plot. [13]

1.3 NiMH battery

Metal hydrides are used as hydrogen storage material, with high hydrogen volumetric capacity and reversible hydrogen absorption/desorption reactions. The large application for gaseous hydrogen storage in metal hydride is in the German submarine serial U212. They are propelled by fuel cells and the hydrogen is stored in large metal hydride tanks. Metal hydride can be used to purify and recover hydrogen from gas mixture. [14,15] They can be used to as thermal sorption compression to covert energy from heat into a compressed hydrogen gas by utilizing the enthalpy change during hydrogen absorption/desorption. The largest commercialized application of metal hydride is, however, as the negative electrode material for rechargeable NiMH batteries. The MH electrode is actually a hydrogen electrode but the hydrogen is stored in a hydrogen storage alloy that also contributes the major part of the electrode with some additional binders and current collectors.
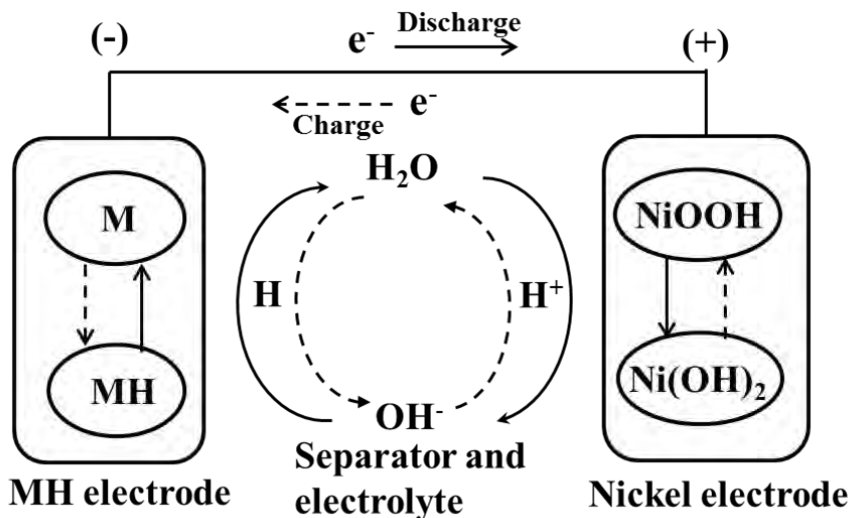
Figure 1.2 Schematic drawing of the electrode reactions in a NiMH battery.

Figure 1.2 depicts the schematic of a Ni–MH battery, containing a metal hydride (MH) electrode and a nickel electrode. In between are a separator and an alkaline electrolyte solution (usually KOH) that provides for the ionic conductivity between the two electrodes. The dashed arrows show the charging reactions and the solid arrows show the discharging reactions. During charging, the nickel hydroxide in the electrode in the positive electrode is oxidised to nickel oxyhydroxide (eq. 1.3), while water in the electrolyte is reduced to hydrogen atoms, which are absorbed by hydrogen storage alloy M in the negative electrode forms hydride MH (eq. 1.4). The reverse reactions take place during discharging. [16]

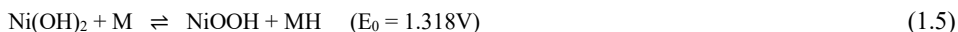The reactions of a NiMH battery can be expressed as;

On the nickel electrode, the reaction is:

$$Ni(OH)_2 + OH^- \rightleftharpoons NiOOH + H_2O + e^- \qquad (E0 = 0.490V) \tag{1.3}$$
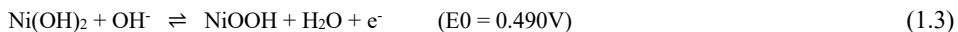
The MH electrode reaction occurring in a NiMH cell is:

$$H_2O + M + e^- \rightleftharpoons OH^- + MH \qquad (E_0 = -0.828V) \tag{1.4}$$

And the overall reaction is:

$$Ni(OH)_2 + M \rightleftharpoons NiOOH + MH \qquad (E_0 = 1.318V) \tag{1.5}$$

The voltage is depending on the O-H bond strength in hydroxide and is around 1.318 V for $Ni(OH)_2$. Although this is substantially lower than the voltage of most commonly used Li-ion batteries, one advantage is that the oxidation potential of metal hydrides is below the oxidation potential of H_2O. So water based solutions can used as electrolyte.

1.4 Overcharge and overdischarge protection

Compared to Li-ion batteries, one big advantage of a sealed NiMH is that it has overcharge and overdischarge protection.[17] The MH electrode is designed to have a higher capacity than the nickel electrode. Therefore, the nickel electrode is the capacity-determining electrode. During overcharging and overdischarging, gas forms by side reactions. The cells are designed to facilitate gas recombination reactions. During overcharging, hydride is continually formed (eq. 1.4), while OH^- ions are oxidized and oxygen evolve at the nickel electrode (eq. 1.6). The oxygen pressure inside the sealed cell starts to rise, and oxygen gas diffuse thought the separator to the MH electrode where it is reduced to water (eq. 1.7).

$$4OH^- \rightarrow O_2 + 2H_2O + 4e^- \tag{1.6}$$

$$4MH + O_2 \rightarrow 4M + 2H_2O \tag{1.7}$$

It should be noted that hydrogen gas also occurs during overcharging when the charge rate is too high to form a hydride or the overcapacity ratio between two electrodes is not high enough (eq. 1.8).

$$2H_2O + 2e^- \rightarrow H_2 + 2OH^- \tag{1.8}$$

Overdischarging

When NiMH batteries are connected in series, small differences in storage capacities might occur. Some batteries can be completely discharged, while others retain some capacity. Continuation of the discharge process will cause overdischarging to those already fully discharged cells. During overdischarging, water is forced to be reduced and H_2 forms at the nickel electrode (eq. 1.9). Advantageously, hydrogen can also transfer through the separator to the MH electrode to be recombined.

$$2H_2O + 2e^- \rightarrow H_2 + 2OH^- \tag{1.9}$$

1.5 Compared to other battery types

Properties of three most used rechargeable batteries are compared in Table 1.2. Compared to NiCd battery, NiMH battery has higher energy density and less of a memory effect. Besides, NiCd battery is not environmental friendly due to toxic Cd. Although NiMH battery has lower energy density and voltage than Lithium-ion battery, it can overcharge and overdischarge with gas recombination reactions as described above. NiMH battery can operate at lower temperature compare to Li-ion battery. NiMH battery is a good choice for the huge demand of vehicle application.

Table 1.2 Comparisons of NiCd, NiMH, and Li-ion Batteries

Properties	NiCd	NiMH	Li-ion
Voltage(V)	1.2	1.2	3.6
Energy density(W·h/L)	50–150	140–300	250–693
Cycle life	2000	500-2000	400-1200
Rate capability	10-20	10	2
Memory effect	Noticeable	Little	No
Operating Temperature(°C)	-30 to +60	-20 to +50	-10 to +50
Cost	Low	Medium	High

1.6 Aim of this thesis

The thesis aims to develop an understanding of metal hydride surface structures for high power NiMH batteries. The automotive industry use of batteries will increase significantly with the introduction of various hybrid solutions for the power trains. In these applications the NiMH battery chemistry is well suited. Höganäs AB and Stockholm University have developed a surface treatment method that improves the reaction kinetics and corrosion stability of conventional NiMH battery AB_5-alloys. A basic understanding of the phenomenon is, however, lacking. With this thesis, we want to increase this understanding, which will form the basis for an extension of the method to include other more available metals, which can be used in batteries.

This thesis presents the background and motivation of the work, explains how experiments are done and how analysis methods are operated, discusses the result from Paper I-IV and make a conclusion of observed results.

2. Experimental and characterisation

2.1 Experimental

2.1.1 Metal hydride alloy samples

A La_{20} Ce_7 Pr_1 Nd_4 Al_2 Mn_5 Co_6 Ni_{55} AB_5-type alloy labelled as K9A was supplied by Inner Mongolia Rare Earth Ovonic Metal Hydride Co, A La_{18} Ce_{10} Pr_1 Nd_3 Al_2 Mn_5 Co_{10} Ni_{51} AB_5-type labelled as B3 was supplied by Santuko. A $Lm(La, Mg, other)$ $Ni_{3.85}$ $Al_{0.15}$ A_2B_7-type alloy labelled as Co-free was supplied by Japan Material & Chemicals Co and A $(Ti_{0.36}Zr_{0.64})$ $(V_{0.15}Ni_{0.58}Mn_{0.20}Cr_{0.07})_2$ AB_2-type alloy was supplied by BASF.

2.1.2 Alkaline treatment

For AB_5-type and A_2B_7-type alloy, the treatment comprises there steps,

The alloy is first decrepitated into smaller particles by a hydriding and dehydriding procedure. This is done by flushing the alloy with hydrogen in a Zirconia (YSZ) tube contained in a stainless steel autoclave under room temperature a few time to remove air. The alloy is then heated under 50 bar hydrogen to 180 °C, thereafter the hydrogen pressure is released to ambient to dehydride the alloy. Then the pressure is increased to 50 bar again to hydride the alloy. This procedure is repeated 10 times leading to uniform temperature swings, indicating a fully decrepitated and hydrided alloy. The step is aim to increase the surface area by reducing the particle size and cause surface segregation which leads rare-earth elements to particle surface as a method of activation.

In order to reduce the risk of igniting the hydrided powder, a pre-oxidation step is done by adding air to the tube to slightly oxidize the alloy after cooling the autoclave to room temperature.

The oxidized alloy powder is then heated in a hot 6M potassium hydroxide solution at 90 °C, different times are tried for different samples. For K9A sample, 3 min, 10 min and 20 min are tried for optimization (see paper I). For B3 and Co-free sample, only 3min is tried. After that the powder is washed with deionized water and dried in vacuum. A passive, but nickel enriched surface layer has been created in this step.

The AB_2-type alloy is only treated in a hot 6M potassium hydroxide solution at 90 °C. The first two steps are not necessary. Due to the strong Zr oxidize shell, 20, 60, 80 and 100 min boiling time are tried. The powder is then washed with deionized water and dried in vacuum. Hot alkaline treatment selectively dissolves elements in particle surface leading to the formation of nickel rich surface layers, also increasing the surface area[18-20]. (see paper II)

2.1.3 Adding oxygen and hydrogen gases to cycled NiMH battery

A NiMH battery construction with access to the internal common gas space makes it possible to manipulate the electrode balance by adding oxygen and/or hydrogen gas. The 0.2 C and 0.9 C-rate capacities of a Nilar NiMH battery are measured as received, and then the measurement is continued with 3 cycles at 0.9C-rate discharge/charge cycling. Just before the end of the last cycle of charging, the internal gas composition is analysed by using ThermoStar gas analysis system from Pfeiffer Vacuum. After that the internal gas space of the battery is evacuated and filled with 3 liter oxygen to

rebalance the electrodes and replenish water in the electrolyte. After 3 discharge/charge cycles, the internal gas is analysed by the same procedure as before. Thereafter 0.2 C and 0.9 C-rate capacities are remeasured. (see paper III)

2.1.4 Recycling of MH-electrode material from NiMH battery

Sonication, ball milling, acid treatment and alkaline treatment are tested to recycle hydrogen storage alloys from spent NiMH batteries. The treatments aim to partially remove the outer corroded surface of the alloy particles while keeping the catalytic properties of the inner surface.

Sonication

The sonication is done by either using an ultrasonic bath or a sonotrode.

2 g of anodic material from cycled Nilar NiMH battery is added in 70 ml of DI water in a 100 mL beaker and a 14 mm sonotrode (Hielscher UP200Ht) is used for sonication. It is sonicated for up to two hours, washed with DI water and thereafter dried by vacuuming.

5 g of cycled anodic material is put in a 25-mL glass beaker, containing 15 mL of deionized (DI) water. The glass beaker is then suspended halfway into the ultrasonic bath and treated for 30 minutes. After the treatment, the acquired light-grey suspension is poured off and the remaining powder rinsed with DI water and dried under vacuum.

Ball milling

20 g of cycled anodic material is ball-milled for 15 minutes with 10 mL of DI water, giving a dark-gray suspension above a layer of electrode material. The liquid content and the suspended particles are poured off and the remaining thick slurry is transferred to a glass frit and washed with DI water. It is then dried under vacuum.

Acid treatment

Sulfuric leaching has been used for rare earths recovery from spent NiMH batteries[21-23]. It is, however, a complicated process. Here we use a low concentration sulfuric solution to remove the corrosion layer on the bulk alloy. 2 g of cycled anodic material is treated by a 30 mL weak sulfuric acid solution (0.05M, 01M and 1M) prepared from a base solution of 95% H_2SO_4 (VWR Chemicals, AnalaR NORMAPUR). After that, it is washed with DI water and dried under vacuum. Dissolution of the rare earth hydroxides can be described as below:

$$2RE(OH)_3 \text{ (s)} + 3H_2SO_4 \text{ (aq)} \rightarrow RE_2(SO_4)_3 \text{ (aq)} + 6H_2O \text{ (l)} \tag{2.1}$$
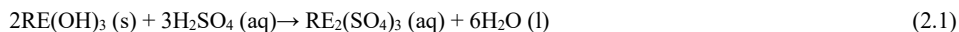
Alkaline washing

2 g of spent alloy is heated in a 20 mL 6 M potassium hydroxide solution at 90 °C for 5 minutes, 10 minutes and 20 minutes, respectively, after which the powders are washed with deionized water and dried in vacuum.

More details of the NiMH recycling experiment are available in Paper IV.

2.2 Characterisation

2.2.1 X-ray Powder Diffraction

The X-ray Powder Diffraction (XRPD) is one of the most widely used scientific techniques for structural characterization of powder materials. X-ray powder diffraction pattern for all samples are obtained with a PANalytical X'pert Pro diffractometer in the Bragg-Brentano geometry[24,25] at 40kV and 40 mA (CuKα_1, λ = 1.5418740 Å). Samples are applied on the flat silicon wafer by dispersing the powder with ethanol which is evaporated before measurement.

2.2.2 Scanning electron microscopy

Scanning electron microscope (SEM) has been widely used to characterize sample's surface morphology by scanning the surface with a focused beam of electrons. Most samples are prepared by dispersing powder on a carbon tape which is stick to an aluminium stub. Scanning Electron Microscopy micrographs and Energy Dispersive Spectroscopy (EDS) data are acquired using a JEOL 7401F Field-Emission Scanning Electron Microscope, a JEOL 7400F analytical SEM setup and a Hitachi TM3000 table top SEM (for particle size assessments). For the cross-section imaging, the powder samples are mixed with conductive carbon cement and polished using a JEOL SM-09010-CP cross-section polisher.

2.2.3 Transmission electron microscopy

Transmission electron microscopy (TEM) is a microscopy technique in which a beam of electrons is transmitted through a specimen to interact with nuclei and electrons of atoms. Therefore it can be used to study small particles in nanoscale. Cross section images of the surface treated alloy are observed by TEM.

2.2.4 Magnetic measurements

A vibrating-sample magnetometer (VSM) is an instrument used to measure magnetic properties. It was invented by Simon Foner at MIT Lincoln Laboratory in 1955 and reported in 1959.[26] The magnetization curves for K9A samples and alkaline treated K9A samples are measured by VSM at Uppsala University.

2.2.5 Surface area measurements

Brunauer–Emmett–Teller (BET) theory explains the physical adsorption of gas molecules on solid surfaces. It establishes the basis for BET method which is a useful analysis technique for the measurement of the specific surface area of materials. Surface area of untreated and alkaline treated samples is measured by BET method at Höganäs AB.

2.2.6 Electrochemistry characterisation

Half-cell test

The working electrode is made by compacting a mixture of 250 mg of alloy powder with 750 mg of Cu powder (200 mesh) or Ni-255 in a tablet press ($\phi = 10$ mm) using a pressure of 210 MPa. A nickel wire is spot welded to the net for electrical connection. A 20 mesh nickel net, spot welded to a nickel wire, is used as counter electrode. A 6 M potassium hydroxide electrolyte is used in the half cell test. A 3 mm zinc rod was used as reference electrode. The discharge capacities of samples are measured in half-cell tests with a Lanhe CT2001A (Land) battery testing instrument.

Resistivity measurement

Resistivity measurement of Nilar battery is done by fully charging the module with 0.1 C for 10 hours followed by rest for one hour. Then it is discharged at 0.5 C for 46 minutes, 0.1 C for 30 seconds, 0.9 C for 30 seconds and 0.5 C for 46 minutes or down to a protective voltage of 10 V. The resistivity is calculated as the ratio of voltage difference to current difference of 0.1C and 0.9C, respectively. Internal resistance is measured every 50th cycle during 0.9 C current cycling. Gas over pressure is measured by a pressure sensor P51-100-A-B-I36-4.5V-R from SSI Technologies Inc. The signal is transferred to voltage and recorded by our computer controlled Land CT 2001A. (1 C = a current equal to the nominal battery capacity divided by 1 h, i. e. a current that will discharge the battery in 1 h).

The capacity check and cycling measured at Nilar are done by a Maccor 4000 Series equipment.

The capacity check and cycling measured at Stockholm University are done by a Lanhe CT2001B (Land) battery testing equipment.

3. Result and discussion

3.1 Surface treatment (Paper I, II)

AB$_5$-type alloys are most common used as materials for the negative metal hydride electrode in NiMH. Newly developed co-free La-Mg-Ni-based A$_2$B$_7$-type hydrogen storage alloys with high discharge capacity have started to enter makes practical applications. AB$_2$-type hydrogen storage alloys are also promising negative electrode materials for rechargeable NiMH batteries; however, suffer from slow activation requiring many charge and discharge cycles for activation. In this work, the alkaline surface treatment method is tried to improve kinetics at surface of metal hydride alloys. The treatment comprises three steps: decrepitating the alloy by cycling it using hydrogen gas; oxidizing the obtained hydride alloy powder and boiling the oxidized powder in an aqueous potassium hydroxide solution. Due to the strong Zr oxidize shell of AB$_2$-type alloy the AB$_2$ alloy is only treated with a hot 6M potassium hydroxide solution at 90 °C. The first two steps are not necessary. Different characterizations are investigated. SEM and TEM characterizations were used to study the surface morphology, three electrodes half-cell tests were used to study the dischargeability. AB$_5$ type alloy is covered with a porous surface layer containing needle shaped rare earth hydroxides after etching by a potassium hydroxide solution. TEM studies show in addition the presence of a denser surface oxide layer with embedded Ni containing clusters covering the bulk alloy. The electrochemical performance correlated to magnetic clusters in metal hydride surfaces after surface treatment is discussed. The result from different characterization methods are presented and discussed below.

K9A alloy

The surface is covered with a needle like phase after treatment (Figure 3.1). The amount of needles grew with the increasing alkaline treatment time, while the size, up to about 1 μm in length, did not show any significant change. This is probably due to an easy nucleation of hydroxides or oxides on the alloy surface. During the treatment, surface segregation occurs; rare earth elements diffuse to surface and Ni containing clusters form[27-30] which are presumably embedded in the denser surface observed under the needle like phase (as seen the high magnification image (d)).
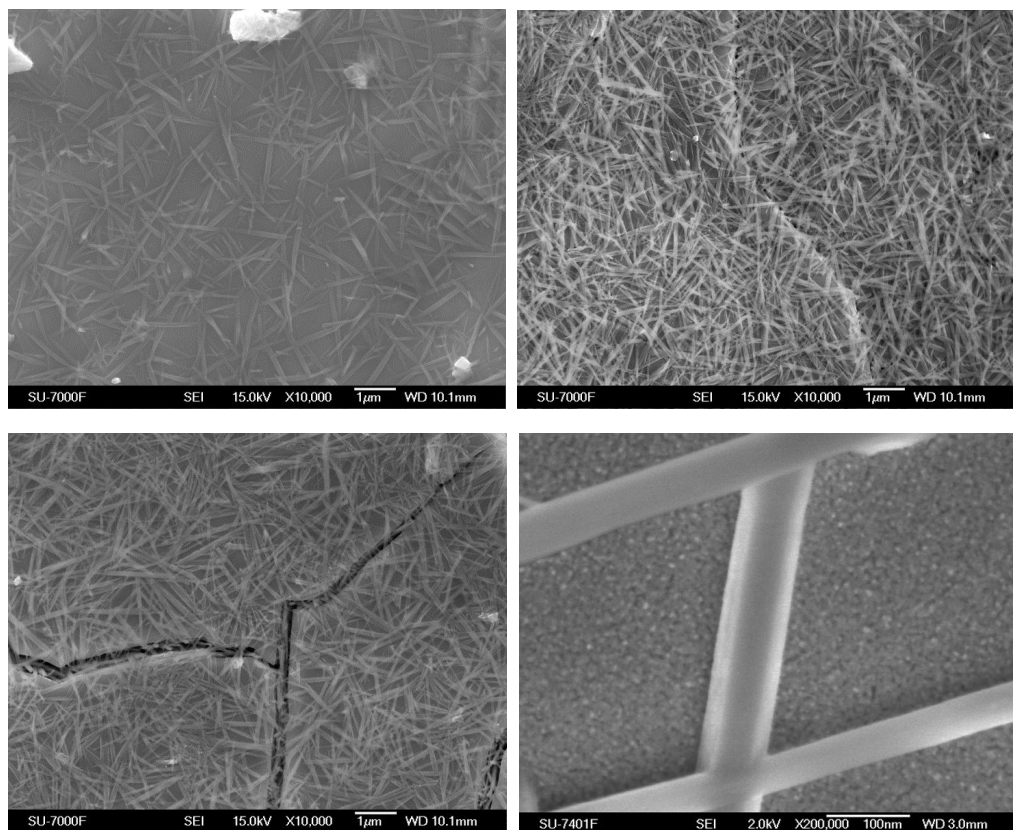
Figure 3.1 SEM images of surface treated K9A alloy surfaces after KOH boiling for 3 mins (a, d), 10 mins (b) and 20 min (c). Figure reproduced from paper I.

Needles were separated from the surface by ultra-sonication and examined under transmission electron microscopy (TEM). The corresponding selective area (a) of separated needles shown in Figure 3.2 was examined by X-ray energy dispersive spectroscopy (EDS). The data listed in Table 3.1 shows that the needle mainly contains oxygen, lanthanum with a small amount of cerium. Rotation electron diffraction (RED)[31-33] was used to collect the single crystal X-ray diffraction pattern of the needle and the reconstructed RED data is shown is Figure 3.3. The suggested space group is P63/m and the La(OH)$_3$ structure could be refined and confirmed by shelxs97[34].

Table 3.1 Summary of the EDS results in atomic percentages for the needle shape phase.

Elements	O	Al	La	Ce
Atomic%	75.58	0.25	19.92	4.25
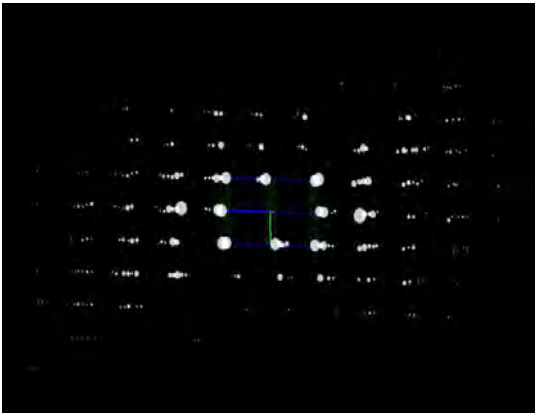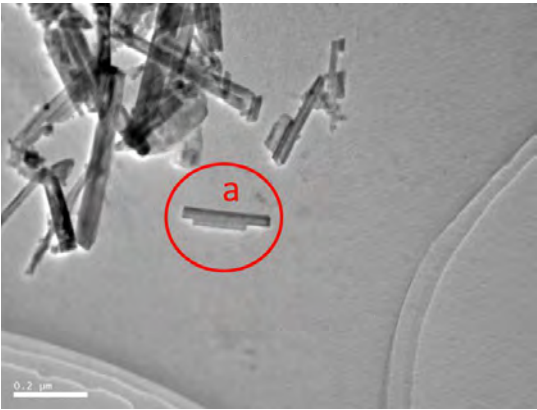
Figure 3.2. TEM image of surface treated alloy after

ultra-sonication and separated needle shape phase (a).

Figure reproduced from paper I.

Figure 3.3. The reconstructed RED data.

The bright-field and dark-field cross section images of the surface treated alloy observed by TEM are shown in figure 3.4. In Figure 3.4b, the un-oxidized metal alloy is marked as A which is coated with a layer of surface oxides (B). Small bright inclusions embedded in the surface oxides layer were suggested to be Ni containing clusters by K. Young et al.[8, 28] These clusters are presumed to contribute to the magnetic properties of surface treated alloy.
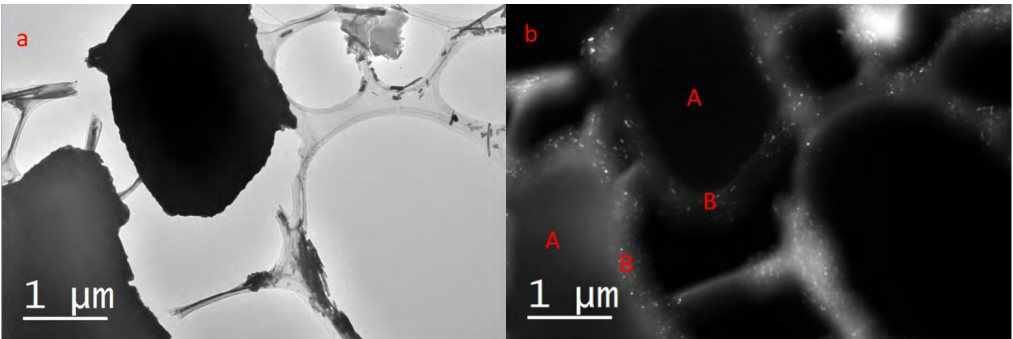
Figure 3.4. TEM bright-field micrograph (a) and dark-field micrograph (b) from the surface treated alloy. Figure reproduced from paper I.

The magnetization curves for the metal hydride before and after surface treatment are shown in Figure 3.5. Paramagentism could be confirmed for the LaNi$_5$-based alloy itself [5, 27, 35, 36]. In addition a small superparamagnetic contribution was observed, probably from an unintentional corrosion of the original alloy. The hydrogen cycled alloy shows an increase of magnetisation at low fields compare to the original alloy, which is due to the addition of a superparamagnetic component caused by nano Ni containing clusters formed during the hydriding/dehydriding cycles. The superparamagnetic component increases with KOH boiling time from 3 to 20 min corresponding to an increased amount of precipitated nano Ni containing clusters. The magnetization curves of alloy after KOH boiling treatment also show an increase of a ferromagnetic component, this is due to a further increased size of Ni containing clusters with etching time. Based on the results we discussed above, the precipitation process of the Ni containing clusters by our surface treatment can be proposed to contain the following three steps: nano Ni containing clusters liberated by the formation of rare earth hydroxides (first step) the amount of Ni containing clusters increases with the treat time (second step) and the size of Ni containing clusters grows with longer boiling in the KOH solution (third step).
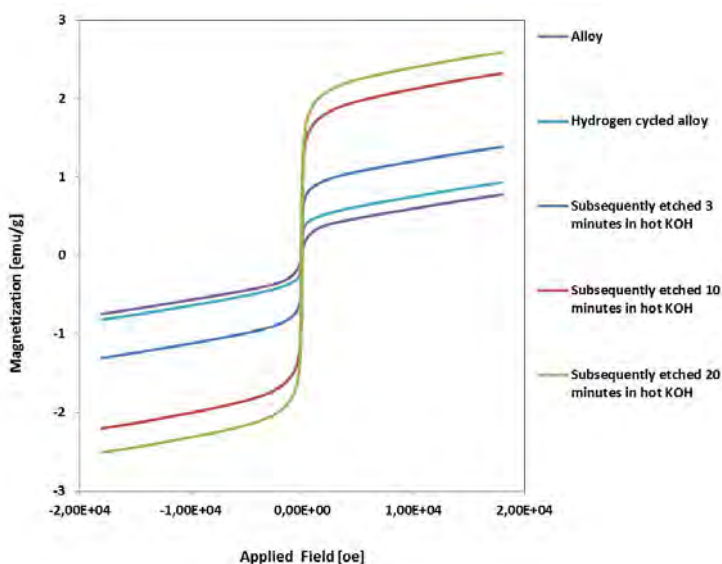

Figure 3.5 The magnetization curves measured at room temperature for the alloy before and after treatment. Figure reproduced from paper I.

The magnetic property of the alloy before and after treatment is investigated. Figure 3.6 shows the discharge voltage vs. capacity curves at different discharge currents of original and surface treated alloy. Discharge capacity at low discharge current (50 mA/g) decreases with the boiling time. This is probably due to the thin passive rare earth hydroxides layer. The effect of Ni containing clusters is more pronounced for high-rate discharge currents. The 3 min treated alloy gives highest discharge capacity at high discharge current (320 mA/g and 640 mA/g). Although more Ni containing clusters formed with the KOH etching time, the amount of passive rare earth hydroxides is also increased, which may reduce the capacity and maybe the Ni containing clusters lose catalytic ability due to the

increased size. Therefore, 3 min KOH boiling time gives the largest surface catalytic activity and shows the best performance.
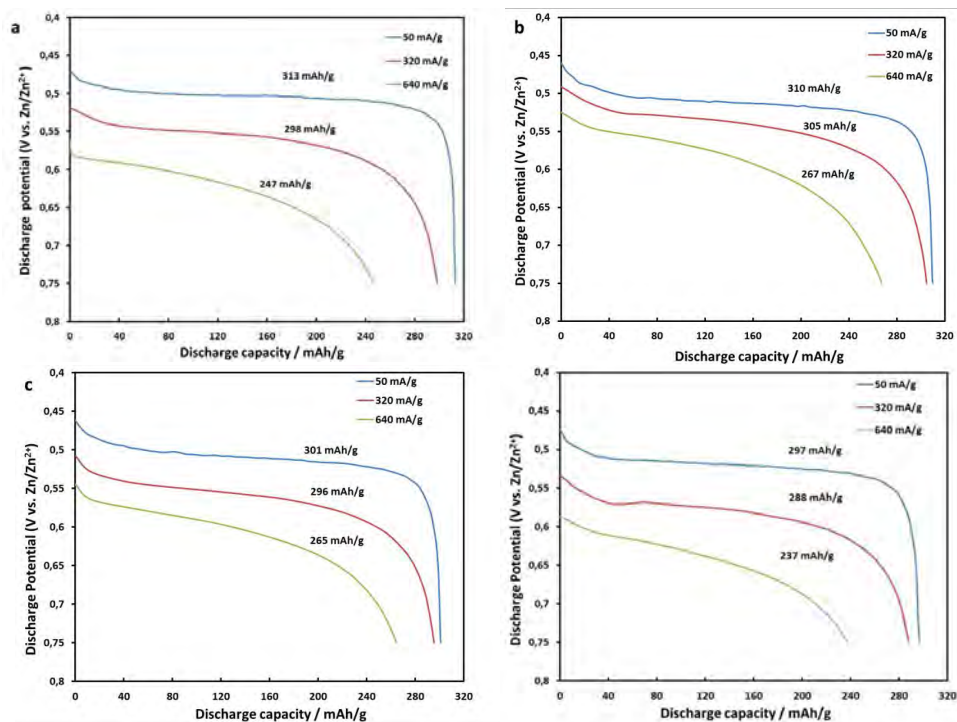

Figure 3.6 The discharge curves at 50 mA/g, 320 mA/g and 640 mA/g for original alloy (a), 3 min KOH boiled alloy (b), 10 min boiled alloy (c) and 20 min boiled alloy (d). Figure reproduced from paper I.

B3 alloy

Short KOH boiling time of K9A alloy gives better performance. So 3min KOH boiling time is tried for the B3 alloy. SEM image of the alloy surface after treatment is presented in Figure 3.7. A needle like rare earth hydroxides phase also here appears on the surface.
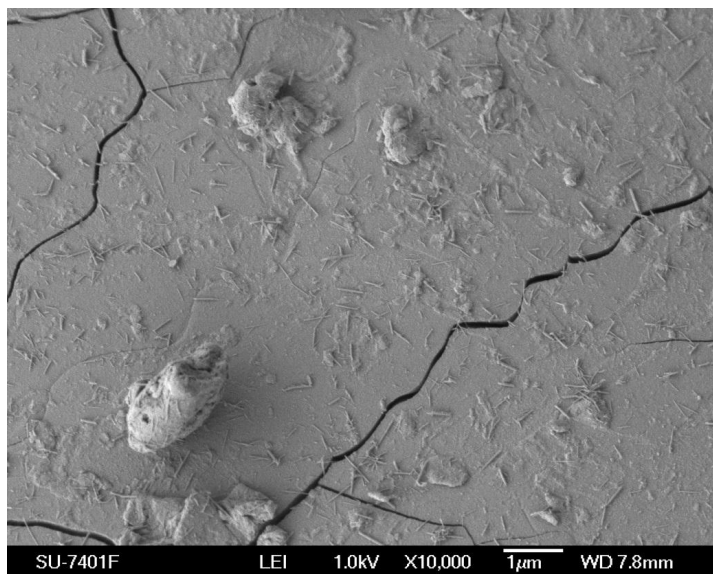
Figure 3.7 SEM images of surface treated B3 alloy surfaces after KOH boiling for 3 mins.

Surface area measured by BET and saturation magnetization (Msat) measured by vibrating-sample magnetometer (VSM) for untreated and treated samples are shown in Table3.2. Surface area of treated alloy is almost double of original alloy, this is due to particle dissertation and oxidized surface layer.

Table 3.2 Surface area of untreated and treated B3 alloy.

Sample	Surface area (m2/g)
B3	0.148
Alkaline treated B3	0.216

Discharge capacity of original B3 and surface treated B3 at different C-rates are shown in Table 3.3. The alkaline treatment also worked for B3 alloy, the high C-rate discharge capacity improved a lot compare to original alloy.

Table 3.3 Discharge capacity of original B3 and surface treated B3 at different C-rates.

Sample	0.2C discharge capacity (mAh/g)	1C discharge capacity (mAh/g)	2C discharge capacity (mAh/g)	4C discharge capacity (mAh/g)	8C discharge capacity (mAh/g)
B3	328	310	263	107	20
Treated B3	323	319	307	251	180

Co-free alloy

Table 3.4 shows the discharge capacity of original Co-free alloy and surface treated Co-free alloy (6M potassium hydroxide, 3mins KOH boiling time at 90°C) at different C-rates. Unfortunately the capacity decreased after treatment, this is probably due to the poor stability of Co-free alloy which is too easily corroded. Probably the result can be improved under a lower KOH concentration or a shorter treatment time. Further characterizations are not done for treated Co-free alloy.

Table 3.4 Discharge capacity of original Co-free alloy and surface treated Co-free alloy at different C-rates.

Sample	0.2C discharge capacity (mAh/g)	1C discharge capacity (mAh/g)	2C discharge capacity (mAh/g)	4C discharge capacity (mAh/g)	8C discharge capacity (mAh/g)
Co-free alloy	335	332	320	280	200
Treated Co-free alloy	256	244	244	184	132

AB2-type alloy

Figure 3.8 shows discharge capacity of original AB_2 alloy and KOH treated AB_2 alloy from 20 min to 100 min. Within 80 min treatment, the discharge capacity increased to around 400mAh/g. The discharge capacity of 100 min treated sample decreased to similar capacity as 20 and 60 min treated samples. This is probably due to surface damage or thicker oxidized layer caused by too long KOH boiling. The activation improved a lot after treatment. The alloy was almost fully activated within the first cycles at the end of the 60 min treatment. The morphology of treated powders was investigation under SEM. The SEM image of 80 min treated sample is given in Figure 3.9. The surface after treatment is extremely rough which increases the surface area and contributes to the fast activation by facilitating the charge acceptance[18].
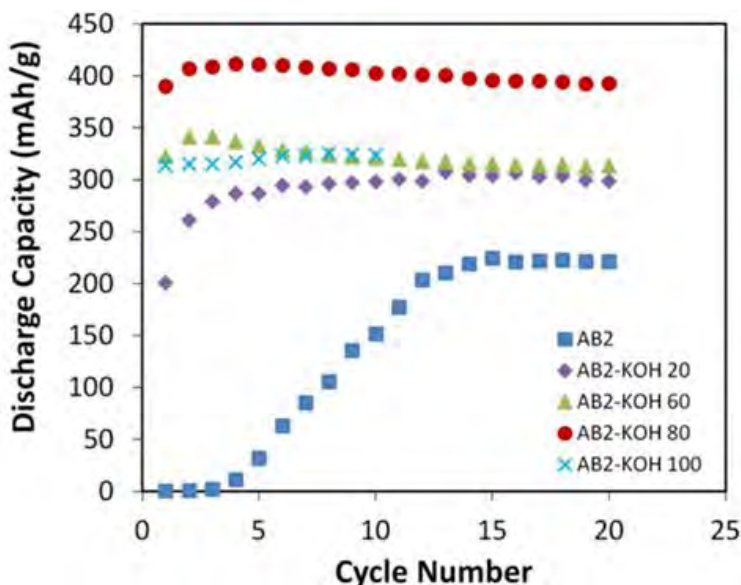
Figure 3.8 Discharge capacity vs. cycle number for original AB_2 alloy, 20, 60, 80 and100 min boiled alloy in 6 M KOH. Figure reproduced from paper II.
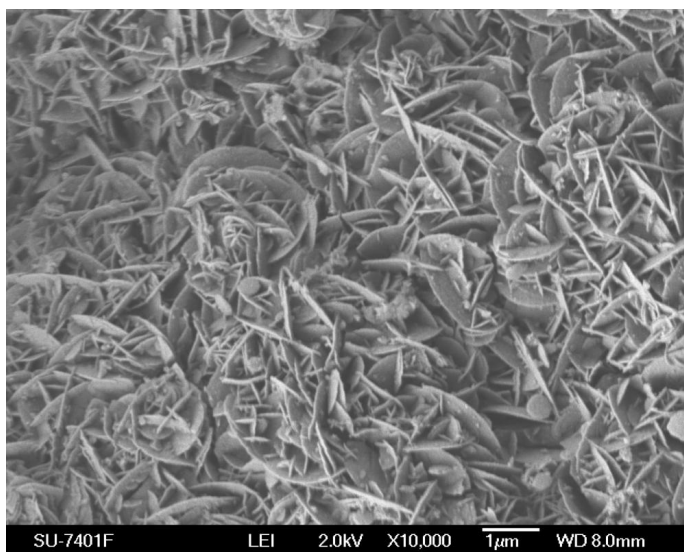
Figure 3.9 SEM image of AB$_2$ alloy after boiling KOH treatment for 80 min.

The treated alloy can be attracted to a permanent magnet whereas the untreated was not. This might due to selective dissolution of alloying elements which leads to the formation of Ni rich surface layers.[19,20] This also contributes fast activation of treated alloy.

For the surface treatment, we want to use a controlled corrosion of the surface of metal hydride particles to improve properties such as activation and kinetics by facilitating the making and breaking of the O – H bond in the water molecules transporting hydrogen in and out of the metal hydride electrode particles. After the surface treatment, a passive rare earth hydroxides layer formed on AB$_5$ alloy and a catalytic interphase surface with embedded nano Ni containing clusters has been created on the alloy surface, which helps to improve high-rate dischargeability. For AB$_2$ alloy, hot alkaline treatment leads to fast activation of alloys yielding a high capacity even without cycling. This high capacity is probably due to the rough surface generated by the alkaline treatment, which could allow higher pressures locally in the powder surface by stabilizing the hydrogen bubbles.[37,38]

3.2 Recovering of cycled NiMH battery performance by adding oxygen (Paper III)

For a NiMH battery, when the cell is formed in the first charge, cobalt, cobalt(II)oxide or cobalt(II)hydroxide added to the $Ni(OH)_2$ electrode is converted to $Co(III)OOH$. This creates both a conductive network and an overdischarge reserve, as the generated hydrogen is absorbed in the MH-electrode alloy [38,39]. In the cell the nickel electrode capacity must be balanced within the limits of the MH-electrode capacity and an open passage for the gas between the electrodes through the separator must be accomplished. So the cell is only filled with a limited amount of electrolyte to allow for gas recombination. Therefore, any subsequent loss of electrolyte after the cells are produced and sealed will degrade performance by increasing the internal resistance. Although Nickel-Metal Hydride batteries (NiMH) have long cycle life, corrosion of the metal hydride is detrimental for life expectancy in the end. Corrosion not only reduces the metal hydride capacity, but also consumes water in the electrolyte resulting in increased internal resistance, which is the main reason caused cell failure. The corrosion also evolves hydrogen, which causes an unbalance between electrodes, increasing the internal pressure when the cells are approaching end of charge. Here, a controlled addition of oxygen is used to rebalance the electrodes and replenish the electrolyte as the added oxygen reacts with hydrogen that was formed during the corrosion process. As the corrosion forms hydroxides with equal molar amounts of both oxygen and hydrogen, a true reconditioning should include equal amounts of oxygen and hydrogen gases. This is to compensate for the loss of oxygen and hydrogen into solid $Mm(OH)_3$. Due to the danger of explosion, oxygen is added at the end of charge and hydrogen is added at the end of discharge. This also protects the alloy from corroding by the pure oxygen. The result from different characterization methods are presented and discussed below.

Figure 3.10 shows the internal resistance of a Nilar NiMH battery measured during cycling with a 0.9 C current. For the first 1000 cycles, the internal resistance/cell increases with increasing number of cycles as the corrosion of the metal hydride consumes the electrolyte. Initially the internal resistance is slightly decreasing with cycling which is attributed to an increasing active surface area as more catalytic nickel containing clusters are formed on the metal hydride particles during the first cycles.[5,9,40] 5 consecutive 3 liter batches of oxygen gas were added after 1000 cycles, the internal resistance decreases dramatically. This is because oxygen recombines to water by oxidizing hydrogen from the corrosion process stored in the metal hydride. The module was again cycled and the increase in resistance following a behavior similar increase in resistivity as in the initial cycling. After another 750 cycles, a second reconditioning by adding 2 consecutive 3liters O_2 and 3liters H_2 batches. This again recovered most of the internal resistance.

As the corrosion forms hydroxides with equal molar amounts of both oxygen and hydrogen, a true reconditioning should include equal amounts of both gases. Thus 3 batches of 2 liter O_2 + 2 liter H_2 were added after 1380 cycles and 2 batches of 2 liter O_2 + 2 liter H_2 were added after 2034 cycles to another module. As shown in Figure 3.12, the module can also be reconditioned.
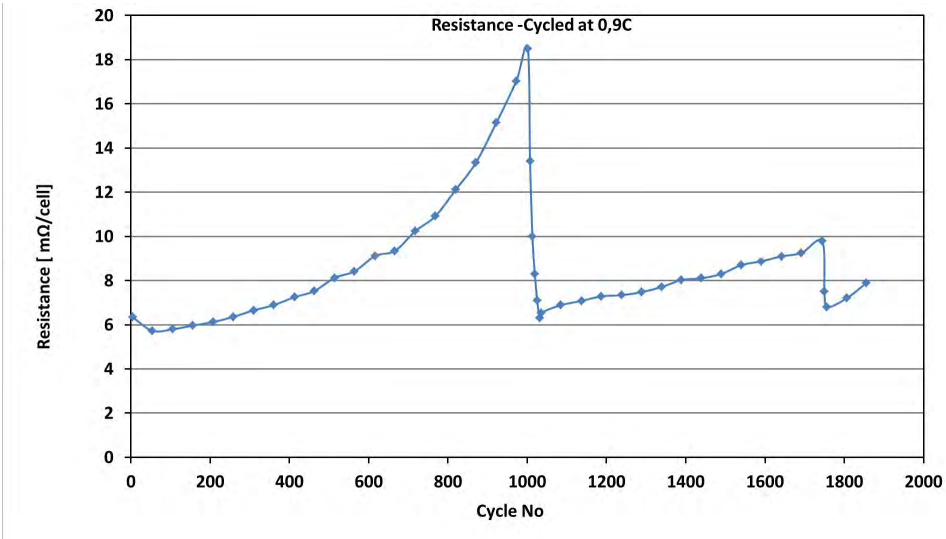
Figure 3.10 Internal resistance measured during cycling with a 0.9 C current. Figure reproduced from paper III.

Figure 3.11 depicts the internal pressure in the module when it is cycled with a 0.5 C current between SOC 20% to 100%. The pressure swings are significantly reduced after an oxygen addition of 3 liters O2.
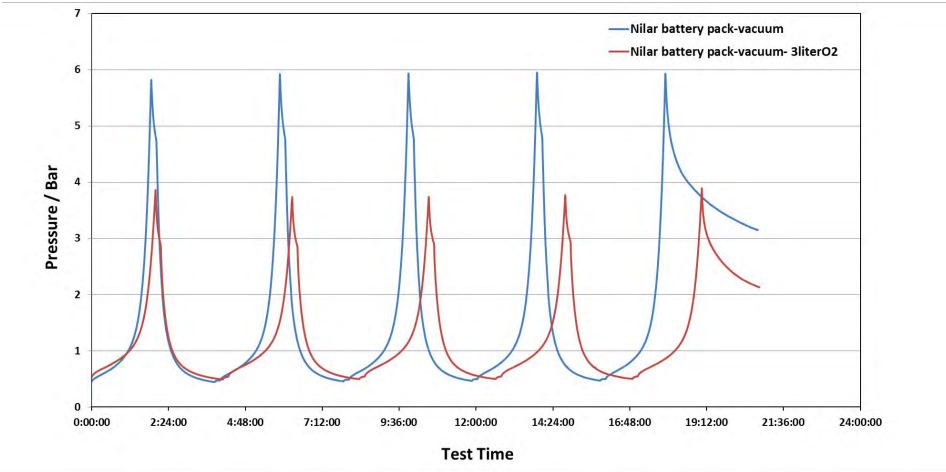

Figure 3.11 Internal gas pressures in a battery module before and after adding 3liter O_2 during cycling with a 0.5 C current. Figure reproduced from paper III.
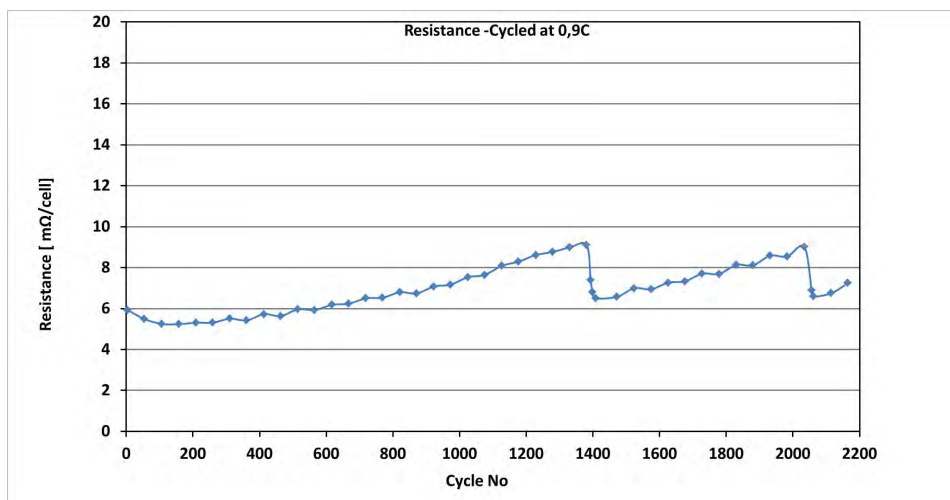
Figure 3.12 Internal resistance measured during cycling with a 0.9 C current. Figure reproduced from paper III.

When the hydrogen storage alloy is slowly corroded during cycling, electrolyte is consumed and electrodes are unbalanced as the corrosion evolves hydrogen. A NiMH battery construction with access to the internal common gas space can be used for manipulating the electrode balance by adding oxygen and/or hydrogen gas. A controlled oxygen addition is used for reconditioning the battery by replenishing water in the electrolyte and rebalances the electrodes mitigating excessive pressures during over charge. Pressure and resistance of the battery are reduced; thereby the cycle life is improved. Both oxygen and hydrogen are added to compensate for the loss to hydroxide ions OH- to fully restore the electrolyte content as well as electrode balance. The oxygen addition should be added when the battery is fully charged or close to be fully charged, because a certain content of hydrogen is needed in the alloy to protect the metals from being oxidized by the oxygen gas. Simple routines can probably be developed to automatically recondition the whole installation, if all cells have access to the same common gas space.[40]

3.3 Regeneration of MH electrode materials from spent NiMH batteries (Paper IV)

In the previous paper, we tried to add pure oxygen gas to an aged NiMH battery pack, to react with the hydrogen liberated in the preceding corrosion process to mitigate the drying out of the cells. We confirmed that the corrosion protection by the initial corrosion during cycling is actually rather effective; most of the alloy is still well protected by the surface after reaching its end of life. This inspired us to try a new method for regeneration of MH-electrode materials by simply cleaning and washing away the passive rare earth hydroxide layer from the cycled powder surfaces. So energy cost of resmelting and recasting of MH-alloys as well as complicated chemical consuming hydrometallurgical processes used in conventional recycling of battery materials could possibly avoid. In this work, the cycled bipolar NiMH battery modules produced by Nilar AB in Sweden are disassembled and the spent MH-electrodes collected. Ball milling, sonication, acid and alkaline treatments are tested to recycle spent alloys from NiMH batteries. Sonication provides a flexible way of treating a system regarding time of interaction, pressures and applied energy[41]. As rare earth hydroxides can be dissolved by acidic solvents, acid treatment is a possible way to remove the passive hydroxides layer. From previous work, we know hot alkaline treatment can improve the electrochemistry performance of AB_2 and AB_5-type hydrogen story alloy[37,42]. Therefore, hot KOH solution is tried to wash away the hydroxide layer. The result from different characterization methods are presented and discussed below.

Mechanical treatments

Figure 3.13 shows the SEM images of the cycled and sonotrode sonicated alloy samples. The needle shape rare earth hydroxide layer can be removed with increasing sonication time.
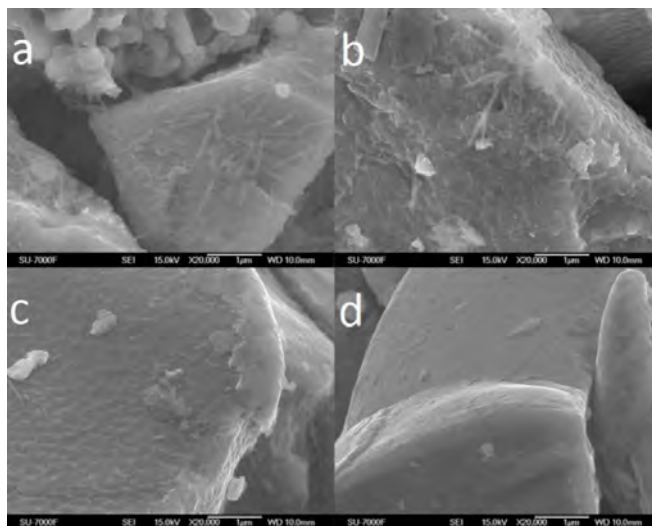

Figure 3.13 SEM secondary electron images at 20000 times magnification. Sonicated samples of cycled anodic material, a) t = 0, b) t = 5 mins, c) t = 30 mins, d) t =2hours. Figure reproduced from paper IV.

Half-cell test result shown in Figure 3.14 indicates an optimum in capacity for the sample with 30mins sonication. The sample with 2 hours sonication showed a lower capacity maybe due to a passivation of the active catalytic species in the surface layer.
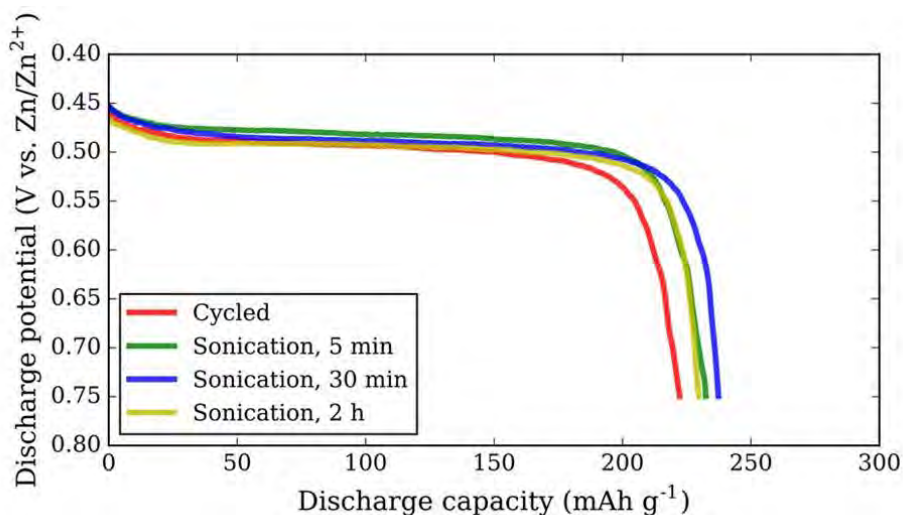

Figure 3.14 The discharge curves at 60 mA/g for cycled alloy, 5 min, 30 min and 2 hours sonication treated cycled alloy, respectively. Figure reproduced from paper IV.

Figure 3.15 shows the SEM images of the cycled material, ultrasonic bath treated and ball-mill treated cycled material. Ultrasonicated and ball-milled material shows very similar surface, with small particle fragments and needle-shaped structures partially covering the surface, which indicates that the rare earth hydroxide layer can be partly removed in an ultrasonic bath as well as by ball-milling.
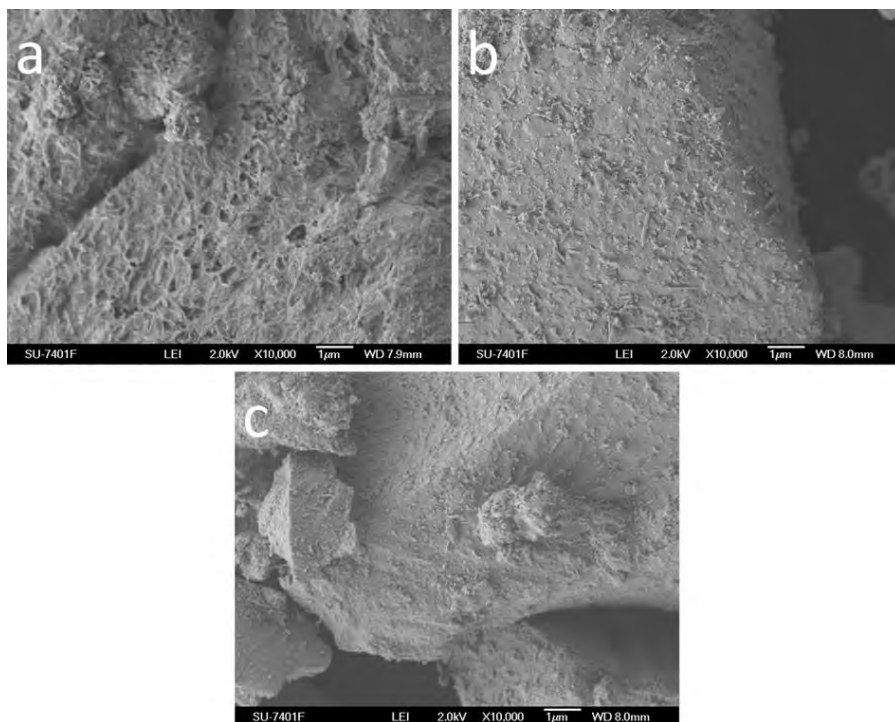
Figure 3.15 SEM micrographs of particle surfaces from; a) cycled material, b) ultrasonicated material, and c) ball-milled material. Figure reproduced from paper IV.

Figure 3.16 shows the first 10 cycles discharge capacity at 60 mA/g current from half-cell test result. The cycled alloy has only lost about 5 % of the initial capacity, showing that most of the alloy capacity remains even if the battery has passed the end-of-life criteria caused by electrolyte dry-out. The ball-milled sample shows the best performance. Not only does it reach the capacity of the pristine alloy but it also shows a very rapid activation. Therefore the active surface created in the formation of the original battery alloy is still remained.
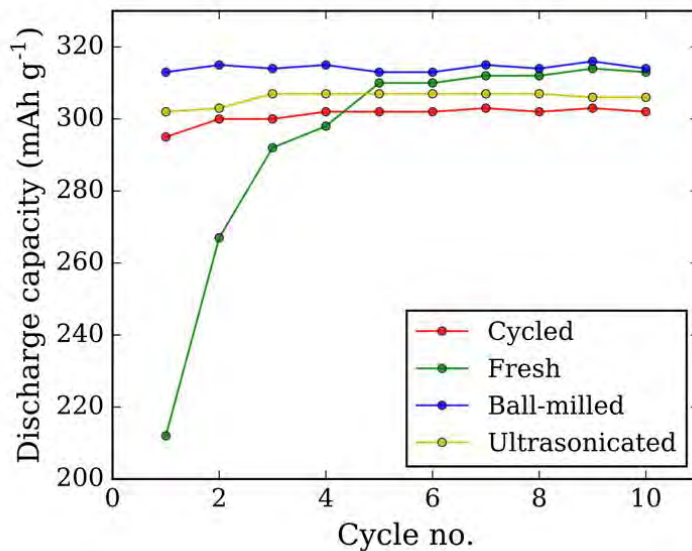
Figure 3.16 Average capacity measured for the first 10 cycles for the treated and untreated samples. Figure reproduced from paper IV.

Chemical treatments

Figure 3.17 shows SEM micrographs of the untreated cycled alloy and of samples treated with different concentration of sulfuric acid. With treatments of all three acid solutions, the rare earth hydroxide needles were removed (Figure 3.17 b, c, d). When the concentration of H_2SO_4 was increased to 1M, the bulk alloy looks like been attacked (Figure 3.17 d). The corresponding half-cell test result is in shown in Figure 3.18a and 3.18b. Discharge capacity of the alloy can be recovered by the treatment of 0.05 M sulfuric acid solution due to removed hydroxides layer. However, with higher concertation of acid solutions, the interface and bulk alloy can be damaged which cause lower capacity and slower activation.
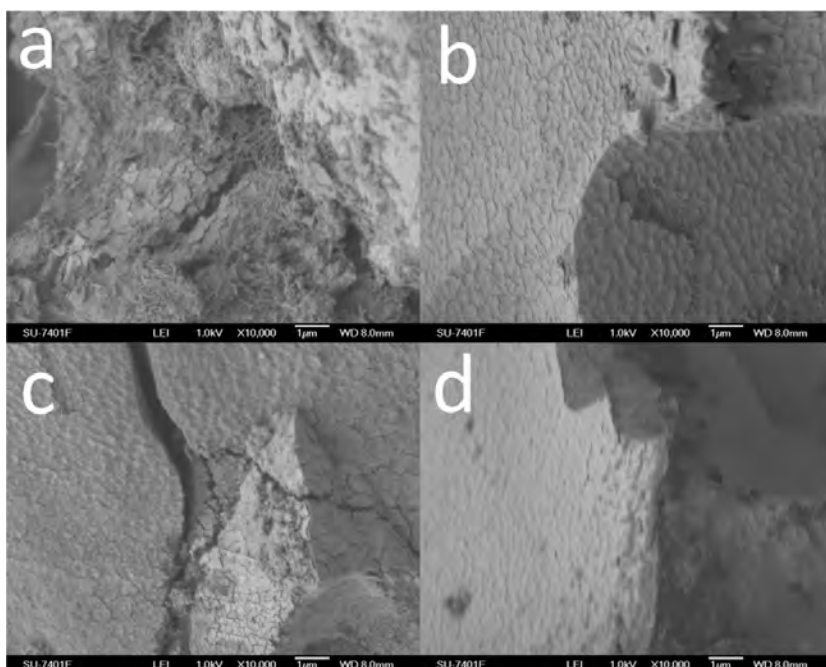
Figure 3.17 SEM secondary electron images at 20000 times magnification. Acid treated samples of cycled anodic material, a) Untreated, b) 0.05M H_2SO_4 for 1 minute, c) 0.01M H_2SO_4 for 1 minute, d) 1M H_2SO_4 for 1 minute. Figure reproduced from paper IV.
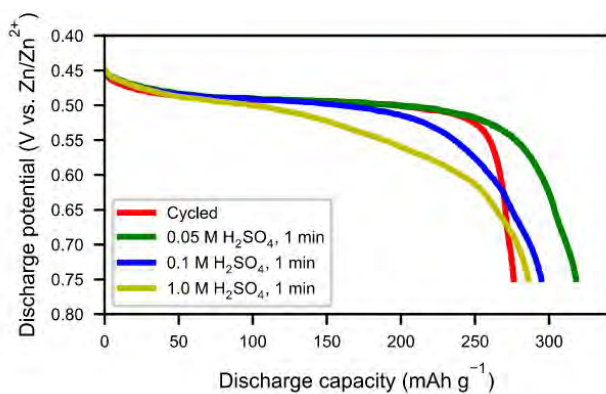
Figure 3.18a The discharge curves at 60 mA/g of cycled anodic material, 0.05M H₂SO₄ for 1 minute, 0.1M H ₂SO₄ for 1 minute and 1M H₂SO₄ for 1 minute treated cycled alloy, respectively. Figure reproduced from paper IV.
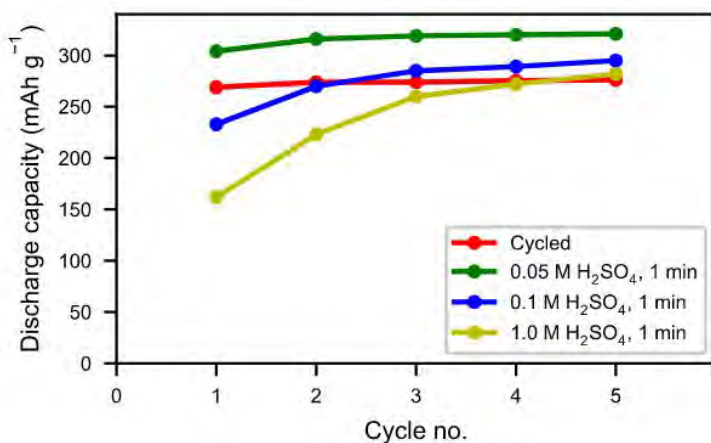

Figure 3.18b Discharge capacity measured for the first 5 cycles for the treated and untreated samples. For all 5 cycles, a discharge rate of 60 mAh g-1 (0.2 C) was used. Figure reproduced from paper IV.

The hydroxide layer cannot be removed within 30 mins hot KOH washing, the layer gets even thicker, which can be seen from SEM images (Figure 3.19) and XRD pattern (Figure 3.20). During the treatment, the size of needle shape hydroxides continues to grow, meanwhile, spent alloy cracks into small particles and the hydroxides layer forms on the new surface.
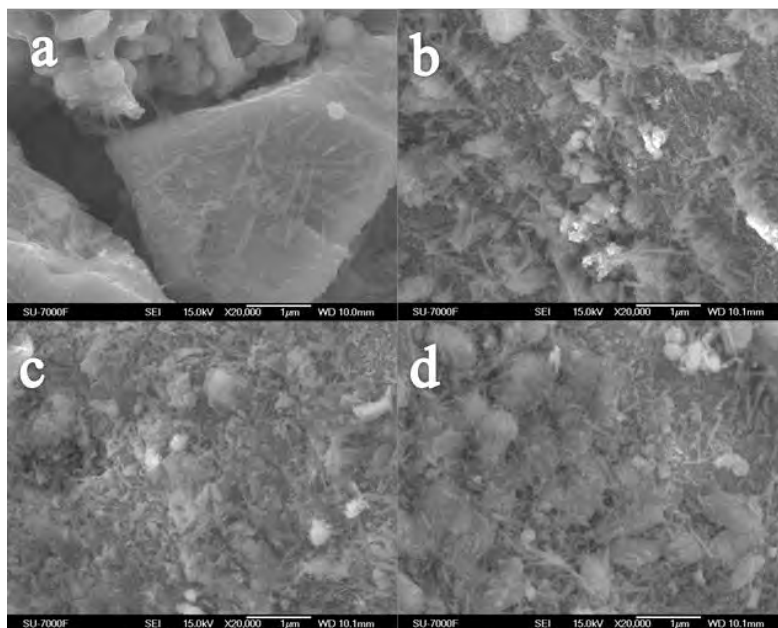

Figure 3.19 SEM secondary electron images at 20000 times magnification. Hot KOH cooking of cycled anodic material, a) t = 0, b) t = 3 mins, c) t = 10 mins, d) t =20mins. Figure reproduced from paper IV.
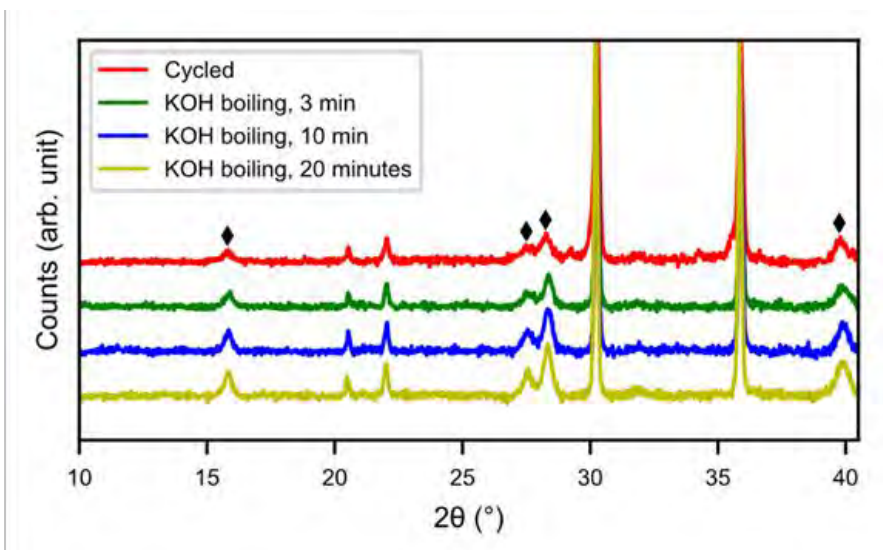
Figure 3.20 XRD patterns of alkaline treated samples, a) untreated, b) t = 3 mins, c) t = 10 mins, d) t =20mins. (◊) La(OH)$_3$. Figure reproduced from paper IV.

Mechanical and chemical treatments are evaluated to recover hydrogen storage alloys from spent NiMH batteries. The corroded rare earth hydroxides layer of cycled alloy can be partially removed by mechanical treatments while still keeping the catalytic properties. The good reaction kinetics is attributed to Ni containing clusters embedded in the interphase and protected by the interphase. Although suitable acid leaching could also remove the corroded layer, it is difficult to control and the whole interphase could also be leached away. Hot alkaline treatment leads to even thicker hydroxide layer. Agglomerated particles of spent alloy with reduced accessibility for the electrolyte can be separated by the mechanical treatment, they become more accessible to the electrolyte and increase the reaction kinetics. Therefore, the recycled MH-electrode material can perform better in its second life in a new battery.[43]

3. Conclusions

Alkaline surface treatment was used to create a controlled corrosion of the surface of metal hydride particles to improve properties such as activation and kinetics by increasing surface area and facilitating the making and breaking of the O-H bond in the water molecules transporting hydrogen in and out of the metal hydride electrode particles. After the surface treatment, although a passive rare earth hydroxides/oxides layer formed, a catalytic surface with embedded nano Ni containing clusters has been created on the alloy surface, which helps to improve the performance of metal hydride alloy.

Corrosion of the NiMH battery will consume electrolyte and unbalance the electrodes as the corrosion evolves hydrogen. The electrode balance of cycled NiMH batteries from Nilar were manipulated by adding oxygen and/or hydrogen gas through the access to the internal common gas space, as the added oxygen reacts with hydrogen that was formed during the corrosion process by replenishing water in the electrolyte. As the corrosion forms hydroxides with equal molar amounts of both oxygen and hydrogen, a true reconditioning should include equal amounts of both gases. Thus, the two most detrimental factors, restore the electrolyte content as well as electrode balance in cell ageing can be mitigated by adding a controlled addition of oxygen and/or hydrogen gas.

Mechanical and chemical treatments were tried to recover hydrogen storage alloys from spent NiMH batteries. The corroded rare earth hydroxides layer of the cycled alloy particles can be partially removed by mechanical treatments while keeping its catalytic properties. It can also be removed by suitable acid leaching. However, treatment with a hot alkaline solution made the hydroxide layer grow thicker. Mechanical treatments sonication and ball-milling lead to a break-up of agglomerated particles, and thereby improving the high-rate properties of the alloy by increasing the access to highly active surface sites. The subsequent density/hydrodynamic separation lead to the removal of corrosion products and smaller particle fragments, giving an increase in capacity. The treated material has an already activated and partially corroded surface; upon partial or full reimplementation into NiMH battery production will consume less of the electrolyte, give longer cycle-life and improve high-rate properties.

Outlook

In this thesis surface treatments have been used to improve the electrochemical performance of metal hydride alloys. More experiments can be done to optimize the procedure for different type of alloys and more characterization techniques can be used to support our hypothesis of the mechanism. A controlled addition of oxygen and/or hydrogen gas to the internal gas space of cycled NiMH battery can recover the battery and increase its cycle life. In the future the reconditioning procedure can be done more frequent during cycling, or when reaching certain inner resistance levels measured in the system. And for the regenerated alloy from MH electrode, it can be partial or full reimplementation into NiMH battery production to give better performance and reduce the cost. NiMH battery is relatively environmental, recyclable and low cost compare to Li-ion battery. If more attention and research can be transferred to the NiMH battery, it will become even better suited for the high demand of automotive industrial use of batteries.
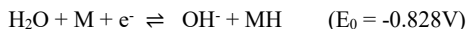
Populärvetenskaplig Sammanfattning

Fordonsindustrins nyttjande av batterier kommer att öka kraftigt i och med införandet av olika typer av hybridlösningar för drivlinor. För dessa tillämpningar passar nickel-metallhydridbatterier väl. Nickel-metallhydridbatterier är återuppladdningsbara och systemet är en nära släkting till nickel-kadmiumbatteriet och nickelvätebatterier, NiH_2, som används i rymdsatelliter p.g.a. sin extremt långa livslängd. Båda systemen, nickel-metallhydrid (NiMH) och nickel-kadmium (NiCd), nyttjar redoxparet $Ni(OH)_2/NiOOH$ som motelektrod, men för NiMH används en vätelagrande legering som anodmaterial istället för kadmium. Kapaciteten för NiMH-batterier kan uppgå till det dubbla av motsvarande NiCd-celler och den volumetriska energitätheten är jämförbar med vissa litiumjonbatterier. Reaktionsförloppet (vid uppladdning) i ett NiMH-batteri kan beskrivas enligt nedan.

För nickelelektroden är halvcellsreaktionen:

$Ni(OH)_2 + OH^- \rightleftharpoons NiOOH + H_2O + e^-$ (E0 = 0.490V)
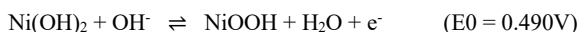
För metallhydrid-elektroden är halvcellsreaktionen:

$H_2O + M + e^- \rightleftharpoons OH^- + MH$ (E_0 = -0.828V)

Den totala reaktionen blir då:

$Ni(OH)_2 + M \rightleftharpoons NiOOH + MH$ (E_0 = 1.318V)

Spänningen som uppnås beror till stor del på bindningsstyrkan för O-H bindingarna i hydroxiden, vilket är cirka 1.318 V för $Ni(OH)_2$. Denna potential må vara påtagligt lägre än spänningen som uppnås i de flesta litiumjonbatterier, men en en fördel med den lägre cellpotentialen är att vattenbaserade elektrolyter kan användas.

Det finns många potentialla hydridinlagrande legeringar, varav AB_2, AB_5, och A_2B_7 är några utav dem. Den vanligaste är AB_5, där A är en blanding av olika sällsynta jordartsmetaller och B i huvudsak nickel. I AB_2 är A titan, vanadin eller zirkonium och B återigen nickel. Generellt sett har AB_2-legeringar en högre urladdningskapacitet än de av AB_5-typ, men kinetiken för AB_2-typer är långsam och de undergår i högre grad korrosion och passiveras därmed lättare. De nyligen utvecklade legeringarna av A_2B_7-typ som är baserade på lantan, magnesium och nickel har även de en hög urladdningskapacitet och de har trots en försämrad cykelstabilitet funnit praktiska tillämpningar. En viktig fördel med legeringar av A_2B_7-typ är att de inte innehåller kobolt, vilket har kommit att bli en dyr del i sammansättningen av både AB_5-legeringar och litiumjonbatterier. Sammantaget är utvecklingen av alternativa material med en kombination av egenskaper, såsom hög kapacitet, fördelaktig kinetik och en god stabilitet vid upp- och urladdning, önskvärda för att förbättre prestandan för NiMH-batterier.

I denna avhandling har bland annat två olika ytbehandlingsmetoder utvecklats, med målet att förbättre kinetiken i yskiktet av metallhydridlegeringen. Behandlingarna kan indelas i tre steg: (1) sönderdela legeringen genom att upprepade gånger ladda upp och ur den med hjälp av vätgas, (2) oxidera det erhållna metallhydrid-pulvret, (3) behandla det oxiderade pulvret genom att antingen koka det i en kaliumhydroxidlösningen eller i form av att tvätta det med väteperoxid. Efter behandingen kan man se att magnetiska kluster av nickel kan återfinnas i ytskiktet av metallhydridpartiklarna. Dessa kluster bidrar till en snabb aktivering och förbättrade höghastighetsegenskaper vid urladdning.

Korrosion i NiMH-batterier leder till att elektrolyten konsumeras och cellerna torkas ut, vilket också skapar en obalans mellan elektroderna i och med den vätgasutveckling som följer. I ett försök att kontrollera detta manipulerades jämvikten mellan elektroder i NiMH-batterier (från Nilar AB) genom att tillsätta syrgas och/eller vätgas till de slutna cellerna. Tillsats av syre bör, tillsammans med den av korrision utvecklade vätgasen, leda till vattenbildning inuti cellen. I och med att korrosionen bildar hydroxider, med lika mängd syre och väte, bör en lika mängd av båda gaserna tillsättas. Därmed kan två skadliga processer, uttorkning och balans mellan elektroderna, avvärjas genom en kontrollerad tillsats av syre och vätgas.

Mekaniska och kemiska tillvägagångssätt för att återanvända legeringsmaterial har prövats. De korroderade beståndsdelarna (mestadels hydroxider av sällsynta jordartsmetaller) kan tas bort med hjälp av mekanisk behandling samtidigt som de goda katalytiska egenskaperna kvarstår. De visade sig även kunna tas bort med hjälp av urlakning med oorganisk syra. Mekaniska behandlingar, med hjälp av ultraljud och malning, ledde till en uppdelning av agglomerat och gav en förbättring av höghastighetsegenskaper vid urladdning. En efterföljande hydrodynamisk separation ledde till att korrosionsprodukter och mindre partiklar uteslöts ur det testade materialet, vilket gav en ökning i kapacitet. Det behandlade materialet visar sig redan vara aktiverat och har en delvis korroderad yta. Detta bör vid implentering i batteriproduktion leda till att mindre elektrolyt konsumeras, vilket bör ge en längre livstid och förbättrade höghastighetsegenskaper.

Acknowledgement

References

[1] In search of the perfect battery, The Economist, 6 March 2008.
http://www.economist.com/node/10789409

[2] Nickel–metal hydride battery,Wikipedia, 12 November 2017
https://en.wikipedia.org/wiki/Nickel%E2%80%93metal_hydride_battery

[3] Taniguchi A, Fujioka N, Ikoma M, Ohta A. Development of nickel/metal-hydride batteries for EVs and HEVs. J. Power Sources, 2001;100: 117-124.

[4] Ye Z, Noréus D, Howlett JR. Metal hydrides for high-power batteries. MRS 2013;38:504-508.

[5] Schlapbach L, Seiler A, Siegmann HC, Waldkirch TV, Zücher P, Brundle CR. Self restoring of the active surface inLaNi5. Int J Hydrogen Energy 1979;4:21–28.

[6] Latroche M, Chabre Y, Decamps B, Percheron-Guegan A, Noréus D. In situ neutron diffraction study of the kinetics of metallic hydride electrodes. J Alloys Compd 2002;334: 267-276.

[7] Broom DP, Kemali M, Ross DK. Magnetic properties of commercial metal hydride battery materials. J Alloy Compd 1999;255: 293 –295.

[8]Young K, Huang B, Regmi RK, Lawes G, Liu Y. Comparisons of metallic clusters imbedded in the surface oxide of AB2, AB5, and A2B7 alloys. J Alloys Compd 2010;506:831–840.

[9] Ye Z, Noréus D. Metal hydride electrodes: The importance of surface area. J. Alloys Compd 2016;664: 59-64.

[10] Chandra D, Chien WM, Talekar A. Metal Hydrides for NiMH Battery Applications. Material Matters Volume 6 Article 2.

[11] Ye Zhou. Metal hydride batteries with AB_5 alloy electrode. Doctoral thesis 2000.

[12] Lototskyy MV, Yartys VA, Pollet BG, Bowman RC. Metal hydride hydrogen compressors: A review. International Journal of Hydrogen Energy 2014;39: 5818-5851.

[13] Martin Dornheim. Thermodynamics of Metal Hydrides Tailoring Reaction Enthalpies of Hydrogen Storage Materials. Chapter from the book Thermodynamics - Interaction Studies - Solids, Liquids and Gases.

[14] Wang QD, Wu J, Chen CP, Ye Z. An investigation of the removal of hydrogen from gas mixtures using misch-metal-based hydrogen storage metals. J Less-common Met 1987;131: 321-328.

[15] Miura S, Fujisawa A, Ishida M. A hydrogen purification and storage system using metal hydride. International Journal of Hydrogen Energy 2012;37: 2794-2799.

[16] Notten PHL, Latroche M. Secondary Batteries – Nickel Systems | Nickel–Metal Hydride: Metal Hydrides. Encyclopedia of Electrochemical Power Sources 2009;4: 494-501.

[17] Ye Z, Noréus D. Oxygen and hydrogen gas recombination in NiMH cells. Journal Power Sources 2012; 208: 232–236.

[18] Liu BH, Jung JH, Lee HH, Lee KY, Lee JY. Improved electrochemical performance of AB2-type metal hydride electrodes activated by the hot-charging process. J Alloy Compd 1996;245: 132-141.

[19] Gao XP, Zhang W, Yang HB, Song DY, Zhang YS, Zhou ZX, et al. Electrochemical properties of the $Zr(V_{0.4}Ni_{0.6})_{2.4}$ hydrogen storage alloy electrode. J Alloy Compd 1996;235: 225-231.

[20] Jung JH, Liu BH, Lee JY. Activation behavior of $Zr_{0.7}Ti_{0.3}Cr_{0.3}Mn_{0.3}V_{0.4}Ni$ alloy electrode modified by the hot charging treatment. J Alloy Compd 1998;264: 306-310.

[21] Pietrelli L, Bellomo B, Fontana D, Montereali MR. Rare earths recovery from NiMH spent batteries. Hydrometallurgy 2002; 66:135-139.

[22] Innocenzi V, Vegliò F. Recovery of rare earths and base metals from spent nickel-metal hydride batteries by sequential sulphuric acid leaching and selective precipitations. Journal of Power Sources 2012;211:184-191.

[23] Li LY, Xu SM, Ju ZJ, Wu F. Recovery of Ni, Co and rare earths from spent Ni-metal hydride batteries and preparation of spherical $Ni(OH)_2$. Hydrometallurgy 2009;100: 41-46.

[24] Brentano J. Focussing method of crystal powder analysis by X-rays. Proc. Phys. Soc 1924;37: 184–193.

[25] Instrument X-ray Optics, I. Reflection Geometry, Birkbeck College, University of London http://pd.chem.ucl.ac.uk/pdnn/inst1/optics1.htm

[26] Foner S. Versatile and Sensitive Vibrating-Sample Magnetometer. Rev. Sci. Instrum. 1959;30: 548–557.

[27] Li HW, Ikeda K, Nakamori Y, Orimo S, Yakushiji K, Takanashi K, Ohyyama H, Nakatsuji K, Dansui Y. Size distribution of precipitated Ni clusters on the surface of an alkaline-treated $LaNi_5$-based alloy. Acta Mater 2007;55: 481–485.

[28] Young K, Chao B, Liu Y, Nei J. Microstructures of the oxides on the activated AB2 and AB5 metal hydride alloys surface. J Alloys Compd 2014;606: 97–104.

[29] Stucki F, Schlapbach L. Magnetic Properties of $LaNi_5$, FeTi, Mg_2Ni and their Hydrides. J Less Common Met 1980;74: 143-151.

[30] Schlapbach L. Magnetic properties of $LaNi_5$ and their variation with hydrogen absorption and desorption. J Phys F: Met Phys 1980;10: 2477-2490.

[31] Zhang DL, Oleynikov P, Hovmöller S, Zou XD. Collecting 3D electron diffraction data by the rotation method. Z Kristallogr 2010;225: 94-102.

[32] Zou XD, Hovmöller S, Oleynikov P. Electron Crystallography - Electron microscopy and electron diffraction. Oxford University Press ISBN: 978-0-19-958020-0;2011.

[33] Wan W, Sun JL, Su J, Hovmoller S, Zou XD. Three-dimensional rotation electron diffraction: software RED for automated data collection and data processing. J Appl Crystallogr 2013;46: 1863-1873.

[34] Sheldrick, GM. A short history of SHELX. Acta Cryst 2008;64: 112–122.

[35] Suzuki K, Ishikawa K, Aoki K. Degradation of LaNi5 and LaNi4.7Al0.3 hydrogen-absorbing alloys by cycling. Mater Trans 2000;41: 581-584.

[36] Tai LT, Hang BT, Thuy NP, Hien TD. Magnetic properties of LaNi5-based compounds. J Magn Magn Mater 2003;262: 485–489.

[37] Shen Y, Peng F, Kontos S, Noréus D. Improved NiMH performance by a surface treatment that creates magnetic Ni-clusters. International Journal of Hydrogen Energy 2016;41: 9933-9938.

[38] Sakai T. Matsuoka M, Iwakura C. Rare Earth Intermetallics for Metal-Hydrogen Batteries Handbook on the Physics and Chemistry of Rare Earths 1995;21: 135-180.

[39] Oshitani M, Yufu H, Takashima K, Tsuji S, Matsumaru Y. Development of a pasted nickel electrode with high active material utilization. Electrochem Soc 1989;136: 1590-1593.

[40] Shen Y, Noréus D, Starborg S. Increasing NiMH battery cycle life with oxygen. International Journal of Hydrogen Energy 2018;43: 18626-18631.

[41] Suslick KS. Sonochemistry. Science 1990;247: 1439-1445.

[42] Tan S, Shen Y, Şahin, EO, Noréus D, Öztürk T, Activation behavior of an AB2 type metal hydride alloy for NiMH batteries. International Journal of Hydrogen Energy 2016;41: 9948–9953.

[43] Shen Y, Grape E, Noréus D, Widenkvist E, Starborg S. Upcycling of spent NiMH battery material - Reconditioned battery alloys show faster activation and reaction kinetics than pristine alloys as well as longer cycle life due to lower corrosion rates. In Manuscript.